Construction and Building Materials 450 (2024) 138720

Contents lists available at ScienceDirect

Construction and Building Materials

journal homepage: www.elsevier.com/locate/conbuildmat

# Hygrothermal and mechanical characterization of novel hemp-lime composites with enhanced consistency

Osamah Mahmood [a,b], Miroslava Kavgic [a,*], Martin Noel [a]

[a] Civil Engineering Department, University of Ottawa, 161 Louis Pasteur, Ottawa, ON K1N 6N5, Canada
[b] Civil Engineering Department, University of Samarra, Samarra, Slah Aldeen 34010, Iraq

ARTICLE INFO

*Keywords:*
Hemp-lime composites
Fine hemp fragments
Hydrated lime
Slag
Hygrothermal properties
Mechanical properties

ABSTRACT

Hemp-lime composites have captured attention in the construction industry due to their sustainability and excellent hygrothermal performance. However, variability and inconsistent performance have hindered their widespread adoption. This research introduces a novel approach to improve the uniformity and hygrothermal characteristics, aiming for reproducibility and consistency comparable to traditional insulation materials. This method included (1) reducing hemp particle size to coarse (1.33 mm), medium (0.92 mm), and fine (0.72 mm) particles; (2) maximizing the hemp proportion to 70 % by weight; and (3) standardizing dry density using vibration techniques. The findings indicate dry density variability reduction in all samples, with a coefficient of variation ranging from 0.16 % to 2.36 %. The hygrothermal analysis demonstrates enhanced insulation and moisture-buffering properties, along with reduced directional disparity in thermal conductivity (1.2–6.8 %) compared to the control sample, particularly in samples with fine particle sizes. Thermal conductivity was within the range of 0.0535–0.0667 W/m K, considerably lower than previously reported values. Also, a positive correlation is observed between moisture-buffering and hemp ratio, indicating that higher hemp ratios in the composite lead to increased moisture capacity, with moisture buffer values of 2.47, 2.28, and 2.12 g/m$^2$ RH corresponding to the binder-to-hemp ratio of 30:70, 40:60, and 50:50 by weight, respectively.

## 1. Introduction

Bio-based construction materials have captured the attention of research and industry sectors over the last decade, mainly due to their carbon sequestration ability and superior hygrothermal properties [1–5]. As such, they pose a sustainable solution for developing an energy-efficient, carbon-zero built environment with a healthy indoor environment [6–9]. Hemp-lime composites (HLC), or hempcrete, are among the most recognized and broadly used bio-based materials globally, consisting of a mixture of hemp shiv, hydrated lime-based binders, and water [9]. Analogous to other bio-based construction materials with high porosity, hemp-lime composites are known to be sensitive to many factors affecting their performance that fall into two broad categories: properties of natural lignocellulosic constituencies (shiv/hurd) and manufacturing or construction approaches [10–13]. In this respect, hemp shiv contains impurities and exhibits highly variable granulations and sizes depending on the decortication process and the industrial hemp variety [13]. Simultaneously, the distribution of hemp shiv particle sizes has a crucial effect on the thermal and mechanical properties of the resulting composite [14].

Several studies investigated the impact of shiv particle size on the hygrothermal and mechanical properties of hemp-lime composites. While they all reported the relevance of this impact, their findings may seem discrepant, raising the need for further investigation of the impact of particle size on hygrothermal and mechanical properties of hemp-lime composites. For example, Brzyski [13] investigated the impact of two hemp shiv sizes on the mechanical and hygrothermal behavior of HLC. Fine shivs, averaging 2.74 mm in length and 1.42 mm in width, were used to create samples with a density of 382 kg/m$^3$, while thick shivs, with an average length of 8.4 mm and 2.68 mm in width, resulted in samples with a density of 377 kg/m$^3$. Their results suggest that the samples with thick shiv exhibited a higher compressive strength of around 0.51 MPa than those with fine particles, which had a compressive strength of approximately 0.40 MPa. Additionally, samples made of thick shiv had higher capillary uptake of 8.82 kg/m$^2$ h$^{1/2}$ compared to 7.27 kg/m$^2$ h$^{1/2}$ for fine shiv. The study reported average thermal conductivity values of 0.105 W/m K for fine shivs and 0.099 W/m K for thick shivs, concluding that HLC with fine shivs has about 6 % higher

* Corresponding author.
*E-mail addresses:* omahm039@uottawa.ca (O. Mahmood), mkavgic@uottawa.ca (M. Kavgic).

https://doi.org/10.1016/j.conbuildmat.2024.138720
Received 18 May 2024; Received in revised form 12 September 2024; Accepted 11 October 2024
Available online 18 October 2024

thermal conductivity than HLC with thick shivs. Another study by Arnaud [15] explored the effect of using hemp shiv of 3.1 mm, 7.6 mm, and 8.9 mm, conforming to dry densities of 390 kg/m$^3$, 400 kg/m$^3$, and 430 kg/m$^3$, respectively, on the mechanical properties of hemp-lime composites. This study concluded that large shivs showed a higher compressive strength when tested at 28 days by about 52.38 % compared with small shivs. However, the study also concluded that the samples with a smaller shiv size produced higher strength by 30.5–50 % than those with larger and medium-sized shivs after 4 months, respectively, as fine shivs were better wrapped with binder particles. Stevulova [14] studied the mechanical and thermal properties of hemp-lime composites using three different shiv sizes of 7.3 mm, 27.7 mm, and 33.7 mm, corresponding to 1150 kg/m$^3$, 1070 kg/m$^3$, and 1040 kg/m$^3$ densities. While their study concluded an increase in compressive strength from 2.73 MPa to 5.20 MPa when particle size reduced from 33.7 mm to 7.3 mm, thermal conductivity values were around 0.11 W/m K regardless of the particle size.

Manufacturing is another crucial factor affecting hemp-lime performance due to the material's anisotropic behavior, which may yield different mechanical and thermal properties based on the direction in which the material is tested [16]. In real-world applications, hemp-lime composites are applied via spraying, casting on-site, or installing precast products (e.g., panels, blocks) [17]. Regardless of the method, the compaction level, the depth of the layer, and the direction of compaction can significantly affect the distribution of density, thermal conductivity, compressive and tensile strength, and capillary rise [4,16–20]. Nguyen [4] investigated the effect of compaction on the mechanical and thermal properties of hemp-lime composites for different densities ranging from 320 kg/m$^3$ to 810 kg/m$^3$ and binder types. The study confirmed previous findings that thermal conductivity and compressive strength have a linear relationship with the density and also concluded that the thermal conductivity of hemp-lime composites tested perpendicular to compaction was 50 % higher than those tested in a direction parallel to compaction. Brzyski [16] also studied the effect of compaction direction on hemp-lime composites' thermal and mechanical properties for two different hemp shiv sizes averaging 2.7 and 8.4 mm and reported a variation in the thermal conductivity values for samples with parallel (0.094 and 0.087 W/m K) and perpendicular (0.105 and 0.101 W/m K) heat flow to the compaction direction. Additionally, the water absorption coefficient in the parallel direction was reported to be 17.6 % and 18.4 % higher than the coefficient determined in the perpendicular direction for 2.7- and 8.4-mm shiv, respectively. Williams [18] studied the effect of the casting process on the mechanical and thermal properties of three hemp-lime layers, 25, 50, and 150 mm, and three compaction levels, 30, 40, and 60 % of volumetric decrease with two sets of tests, one parallel to compaction and one perpendicular to it. The study showed that the layer thickness did not significantly impact the hemp-lime composite properties. In contrast, an increase in the compaction level from 30 % to 60 % increased thermal conductivity by 16.5 % and 8.4 % for perpendicular and parallel directions, respectively. The results also showed a linear relationship between thermal conductivity and compaction level.

Furthermore, Holcroft et al. [2] investigated how different compaction levels affect the moisture buffering capacity of HLC. Their study used a 1-part hemp shiv ratio to 1.65 parts lime binder, creating samples with densities ranging from 210 kg/m$^3$ to 333 kg/m$^3$. These densities were achieved by compacting the samples with weights varying from 1 kg to 10 kg. The study found that the sample with the lowest density had the highest moisture buffering value (3.06 g/m$^2$ RH). This value decreased by just 6 % when the density increased to 278 kg/m$^3$ but fell by 39 % at the highest 333 kg/m$^3$ density. Additionally, Collet et al. evaluated the effect of the manufacturing method on the hygric behavior of HLC [11]. The study considered three types of HLC for wall construction, where each type varies in composition and manufacturing technique: precast, sprayed on, and molded, with average produced densities of 460, 430, and 430 kg/m$^3$, respectively. The study showed that the moisture buffering values were 1.94, 2.15, and 2.15 gm/m$^2$ RH, corresponding to precast, sprayed-on, and molded samples. The study also indicated a negative correlation between HLC density and moisture buffering value.

The literature review indicates that hemp-lime composites' mechanical and hygrothermal properties significantly vary depending on the hemp particle size, orientation, and compaction level, hindering their reproducibility and consistent quality. Commercial, large-scale application of hemp-lime composites requires natural constituent properties and manufacturing procedures to be standardized and easily controlled. This study addresses these challenges by proposing a new integrated approach combining uniformly reduced-in-size hemp shivs with vibration as a casting process to produce consistent quality and performance hemp-lime samples. Hence, this is the first study to address the following critical research objectives: (i) to combine finely ground hemp particles and vibration techniques to develop consistent hemp-lime composite materials, (ii) to investigate the impact of uniformly reduced hemp shiv particle sizes obtained through a grinding process on the hygrothermal and mechanical performance of hemp-lime composites, (iii) to evaluate the effectiveness of the vibration process in producing hemp-lime samples with consistent physical properties, and (iv) to decrease the hemp-lime composites' thermal conductivity and carbon footprint through the increased content of natural constituencies. Hemp-lime samples were created using hemp shives that were ground to four different particle sizes (D90 of 4.52, 1.33, 0.96, and 0.72 mm) and three different binder-to-hemp ratios (1:1, 1:1.5, 1:2.4). All hemp-lime samples were manufactured through a vibration process to achieve three different target dry densities within a tolerance of +/-3.5 %. The samples' hygrothermal and mechanical behaviors were experimentally investigated following relevant standards.

## 2. Materials and methods

### 2.1. Hemp shiv

The hemp-lime samples were created from hemp shiv, hydrated lime, slag, and water. The hemp shivs used in this study were provided by a local Canadian producer (Terrafibre). Four types of hemp shiv with different fractions were considered in this study, as shown in Fig. 1-a. The first type was the received (R) shiv, while other types were reduced in size to various degrees: coarse-size (C), medium-size (M), and fine-size (F), produced by grinding the received shivs using an industrial grinder (JTANGL Electric Grain Grinder Mill, 3000 W).

### 2.2. Characterization techniques

Various approaches have been employed in the literature to characterize hemp shiv [19]. A laboratory investigation by [20] on establishing characterization methods for hemp shiv demonstrated strong repeatability [19]. Consequently, this study adhered to the prescribed protocols [21] for assessing density, water absorption, particle size distribution, and moisture content.

#### 2.2.1. Bulk density

The bulk density was determined using the following procedure. Firstly, enough material was selected to fill out at least half of the cylindrical mold expected to be used to measure the bulk density. Secondly, the material was oven-dried at 60 °C using a convection oven fitted with an extraction fan to remove the humidity until a constant mass was achieved when the variation between two consecutive readings at 24 h was less than 0.1 %. Then, the sample was placed in a sealed plastic bag until it reached room temperature. Then, the shivs were placed in the cylindrical mold to reach half of the volume of the cylinder. After that, the cylinder was upended ten times and shaken to achieve a horizontal surface. The following step included marking the level of the shiv in the cylinder and then removing the shiv from the mold to

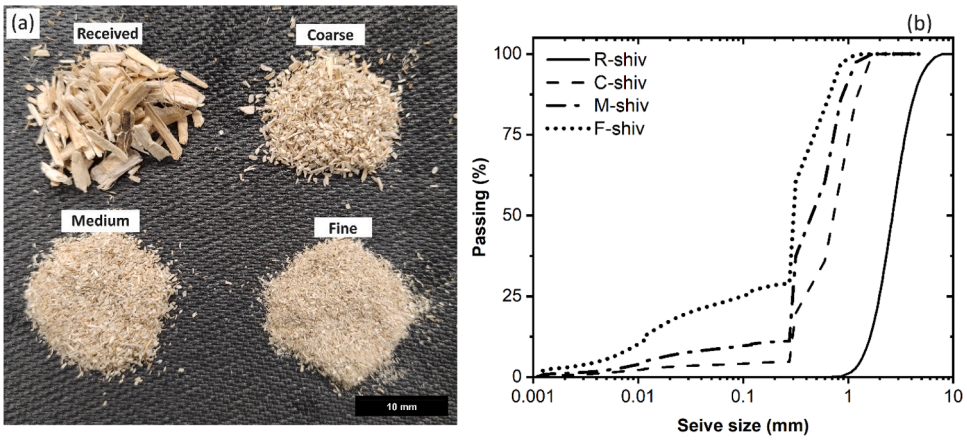


**Fig. 1.** Hemp shivs that were used in this study (a) and their particle size distribution were determined by image analysis, mechanical sieving, and laser diffraction (b).

determine the mass of the sample. Finally, the occupied volume was determined by filling the mold with water up to the previously marked level and measuring the weight of the water. The test was repeated three times with three different samples of shiv. The bulk density was calculated using Eq. (1) [21]:

$$\rho = M/V \tag{1}$$

Where $\rho$ is the bulk density, $M$ is the mass of the shiv, and $V$ is the sample volume.

### 2.2.2. Moisture content

The following procedure was followed to determine the initial moisture content in the hemp shiv. A sample of 200 gm of hemp shiv was selected. Subsequently, the sample was oven-dried at 60 °C until a constant mass was achieved when the variation between two consecutive readings at 24 h was less than 0.1 %, and the dry mass of the sample was determined. The test was repeated three times with three different samples of shiv. The bulk density was calculated using Eq. (2) [21]:

$$W = 100 \times (m_0 - m_d)/m_d \tag{2}$$

Where $W$ is the initial water content, $m_0$ is the initial mass of the sample, and $m_d$ is the dry mass of the sample.

### 2.2.3. Water absorption

The following procedure is used to assess water absorption in the hemp shiv. Initially, a 25 gm of hemp shiv sample was selected. Then, the sample underwent oven-drying at 60 °C until reaching a consistent mass, indicated by a variation of less than 0.1 % between two consecutive readings taken 24 hours apart, and their dry mass was measured. Subsequently, the sample was submerged in a plastic pail filled with water for 1 minute. After that, the water in the pail was drained, the sample was placed in a "salad spinner" and turned 100 times at a rate of 2 rotations per second. Finally, the weight of the spun sample was determined. The same steps were repeated using another 25 gm of sample but with different immersion times of 15, 240, and 2880 minutes. The test was repeated 3 times with 3 different samples of shivs. The absorption (water content) value using Eq. (2) was determined each time. The initial rate of absorption, measured at 1 minute, and ($K_1$) representing the absorption curve's slope as a logarithmic time function was determined. The water absorption at any given time ($W_t$) was calculated using Eq. (3):

$$W_t = \mathrm{IRA} + K_1 Log(t) \tag{3}$$

Where $W_t$ is the water absorption at any given time, IRA is the initial rate of absorption, and $K_1$ is the slope of the absorption curve.

### 2.2.4. Fiber content

It is essential to report the purity level of the hemp shiv used to produce HLC because hemp fiber content can affect the properties and performance of the HLC [55]. To the authors' knowledge, no standards exist that directly report how to measure the fiber content in the hemp shiv. Therefore, a new methodology was developed to measure the fiber content. This methodology was developed based on the flotation technique, as it is widely used in industries where materials can be separated through density differences caused by the difference in absorption rate between hemp shiv and fibers. The methodology's effectiveness in determining fiber content was assessed through previous testing using hemp shiv samples with different fiber contents ranging from 2 % to 44 %, and the results were crosschecked using a handpicked method where fibers were separated manually from the shiv. The proposed method predicted the fiber content within ±5 % of the results obtained from the handpicking method.

A 10 gm hemp shiv sample was selected to determine the fiber content. Then, the sample was oven-dried at 60 °C until a constant mass was achieved when the variation between two consecutive readings at 24 h was less than 0.1 %, and the dry mass was measured. After that, the sample must be ground to achieve the desired length (2–5 mm). This step can be skipped if the particle size matches the desired length. Subsequently, the sample was entirely submerged in a plastic pail containing 3 liters of water at room temperature. The sample was then stirred for 5 minutes using a magnetic stirrer at medium speed (750 RPM) and left to settle for another 10 minutes. The floating hemp shiv particles were then removed using a fine mesh strainer. The remaining part of the sample in the pail was sieved through sieve No.200 (75 μm), and what was left on the sieve was placed in a container and transferred to a drying oven at 60°C until a constant mass was achieved when the variation between two consecutive readings at 24 h was less than 0.1 %, and the dry mass of the fibers was measured. The fiber content was calculated using Eq. (4):

$$f_c = 100 \times m_f/m_d \tag{4}$$

Where $f_c$ is the fiber content, $m_f$ is the dry mass of the fibers and $m_d$ is the dry mass of the sample.

### 2.2.5. Particle size distribution

The particle size distribution of the received (R) shiv was obtained using the image analysis method to determine the shiv's parameters, including length, width, Feret's diameter, and area [22]. The analysis procedure was conducted on 5 gm R-shiv samples, and the Feret's diameter, representing the diameter of the smallest circle that confines the shiv particle outline, was the default output of the image analysis software ImageJ [23]. Meanwhile, (C), (M), and (F) shiv particle size

distribution was determined using a combination of mechanical sieving for particles bigger than 0.3 mm and laser diffraction for particles less than 0.3 mm, as there was a limitation on detecting the larger particle sizes with laser diffraction apparatus. Fig. 1-b shows the particle size distribution, and Table 1 summarizes the physical properties of the hemp shiv used in this study. The sieve sizes at which 90 % (D90) of the total particles pass were 4.52, 1.33, 0.96, and 0.72 mm, and the sieve sizes corresponding to 50 % pass particle sizes (D50) were 2.59, 0.74, 0.54, and 0.30 mm for R, C, M, and F shiv particles, respectively.

### 2.3. Binder mix design

Before preparing the HLC samples, a pilot study was carried out to examine the effects of incorporating by-products and locally available pozzolanic and cementitious materials at various replacement ratios and different water-to-binder ratios on the physical and mechanical properties of the lime binder. The results indicated that a binder containing 20 % slag and a 100 % water-to-binder ratio exhibited the best mechanical performance compared to the other mixtures. Therefore, the binder mix design included hydrated lime, in compliance with the ASTM C207–18 [24] standards, at an 80 % ratio, and slag, in compliance with ASTM C989/C989M-18a [25], at a 20 % ratio of the total binder weight. Table 2 summarizes their chemical composition and physical properties.

The use of hydrated lime in the formulation offered several advantages. First, hydrated lime has a high pH level, making it suitable for preventing biological corrosion when used with organic materials [13]. Second, lime's large surface area (see Table 2) due to its fine particle size and ability to regulate the pH levels within the mixture [26] promoted optimal conditions for forming stable mineral bonds between hemp shiv and lime, thus enhancing the resulting material's cohesion and strength. Third, hydrated lime aids in carbonation, whereby carbon dioxide from the atmosphere reacts with lime during curing, forming calcium carbonate and effectively sequestering carbon, enhancing the material's sustainability and durability. Nevertheless, because hydrated lime gains strength through slow carbonation progress, the binder formulation was enriched with slag, a by-product of metal smelting processes, and a cementitious material that provides early strength and moisture resistance [26,27]. The addition of slag offered the following benefits. First, high silica content in slag improved cohesion within the hemp-lime matrix, resulting in increased compressive strength and reduced brittleness. Additionally, using slag in hemp-lime composite increased sustainability by diverting industrial waste from landfills and reducing the environmental footprint associated with traditional construction materials.

### 2.4. Composition and preparation of hemp-lime specimens

This study aimed to produce hemp-lime composites with consistent performance, high thermal resistance, and a minimized environmental impact, suitable for sustainable buildings exposed to cold climates. This aim was achieved by (i) maximizing the share of hemp shiv using binder-to-hemp (B/H) ratios of 1:1, 1:1.5, and 1:2.4, (ii) producing lightweight samples with dry densities of 140 kg/m$^3$, 170 kg/m$^3$, and 200 kg/m$^3$, and (iii) using a mechanical process to manufacture uniform samples with consistent dry density.

**Table 1**
Physical properties of four hemp shiv types.

| Property | Hemp shiv type | | | |
|---|---|---|---|---|
| | Received | Coarse | Medium | Fine |
| Bulk density (kg/m$^3$) | 94 | 104 | 107 | 114 |
| Initial moisture content (%) | 7.20 | 6.94 | 7.38 | 7.52 |
| Hemp fiber content (%) | 8.91 | 8.32 | 9.03 | 9.12 |
| Water absorption | | | | |
| IRA % | 150.08 | 137.26 | 142.91 | 139.91 |
| $K_1$ | 47.42 | 51.88 | 52.94 | 52.79 |
| *D90 (mm) | 4.52 | 1.33 | 0.96 | 0.72 |
| **D50 (mm) | 2.59 | 0.74 | 0.54 | 0.30 |

* 90 % of the total particles are smaller than the specified sizes.
** A cumulative 50 % point of diameter (or 50 % pass particle size).

Table 3 summarizes the mix ratios and percentages by mass of hemp-lime samples produced from four types of shiv particle sizes (R, C, M, and F) using three B/H ratios (50/50, 40/60, and 30/70). It should be mentioned that it was unfeasible to create a robust sample with a 1:2.4 (30/70) ratio with the R-shiv received from the manufacturer because the samples kept collapsing when demolding and handling. This finding indicates that reducing and standardizing the shiv particle size is necessary to increase the share of the bio-based component in the hemp-lime mix design. Such behavior could be attributed to the improved cohesion forces, contact, interfacial bonding, packing, and connection between the lignocellulosic particles and the cementitious binder by reducing hemp particle sizes and enhancing homogeneity. Simultaneously, voids and gaps were reduced, resulting in a more robust and compact material less prone to collapse, even with a hemp content of 70 %. Furthermore, the hygroscopic nature of hemp shivs helps regulate moisture levels within the material, contributing to a healthier indoor environment and moisture management by absorbing excess moisture and releasing it when humidity levels decrease. Nevertheless, the hygroscopic properties of hemp shiv can lead to the binder's incompletion of the hydration process. Hence, the quantity of water incorporated into the mixture was calculated considering both the requisite amount for binder hydration and the water absorption capacity of the hemp shiv.

The preparation of the samples included placing the hemp shiv in a plastic pail and adding the binder mix composed of hydrated lime and slag. A hand-operated drill mixer was used for the dry components for 3–4 minutes until a homogenous mixture was achieved. The water was then added to the dry components, and further hand-operated mixing was applied for another 10 minutes to ensure that the moistened binder encapsulated all shiv particles. Fine hemp particles allowed easier mix preparation and more uniform samples than the received hemp shiv product. Considering the lack of standards to measure the workability of the hemp-lime composites, a "test ball" procedure was followed where the mixture was stuck together in hand, forming a ball without excess water, as shown in Fig. 2-b. Since most previous studies that manually produced hemp-lime samples reported significant variations in the density [18,28], the vibration technique was chosen to ensure consistent properties of the hemp-lime samples. Hence, when a desired mixture was obtained, the molds were filled, placed on a vibration table, and vibrated for 30 seconds using 60 Hz frequency to achieve the targeted wet density, as shown in Fig. 2. It is important to note that a preliminary study was conducted to determine the maximum density that could be achieved using vibration before stratification occurs. In this respect, depending on the B/H ratio, the maximum target dry densities achieved by vibration were 200 kg/m$^3$, 170 kg/m$^3$, and 140 kg/m$^3$ for 1:1, 1:1.5, and 1:2.4, respectively. The decrease in dry density corresponds to the increase in the share of hemp shiv with consistent vibration technique applied to all samples.

Two mold shapes were utilized to assess the hemp-lime samples' hygrothermal and mechanical properties. In this respect, 160 mm (width) X 160 mm (length) X 80 mm (height) samples were used to measure the thermal conductivity, specific heat capacity, thermal diffusivity, and moisture buffering potential. Additionally, cubic samples (100 mm×100 mm X 100 mm) were used to measure the compressive strength. As fresh hemp-lime composites have marginal strength, the mold size can affect the de-molding process, as samples might collapse while removed from the mold. Therefore, samples cast for compressive strength were de-molded immediately, whereas other larger samples for hygrothermal tests were de-molded after 48 hours.

Samples were placed in a curing chamber for 28 days under 70 % RH and 22±1 °C temperature until testing. Samples intended for thermal conductivity, specific heat, thermal diffusivity, and moisture buffering value analysis were oven-dried at 65–80 °C until a constant weight was

**Table 2**
The chemical composition and physical properties of hydrated lime and slag.

| Material | Chemical composition | | | | | | | | | Physical properties | |
|---|---|---|---|---|---|---|---|---|---|---|---|
| | Mass % | | | | | | | | | | |
| | CaO | $Na_2O$ | MgO | $Al_2O_3$ | $SiO_2$ | $P_2O_5$ | $K_2O$ | $TiO_2$ | $Fe_2O_3$ | Specific gravity | Surface area g/$m^2$ |
| Hydrated lime | 67.56 | 0.05 | 0.42 | 0.04 | 0.75 | 0.02 | 0.03 | 0.02 | 0.11 | 2.39 | 13.72 |
| Slag | 37.82 | 0.37 | 11.82 | 10.20 | 36.80 | 0.00 | 0.49 | 1.43 | 0.43 | 2.74 | 1.63 |

**Table 3**
Composition of the hemp-lime samples.

| B/H ratio | *Name | Mix % by mass | | | |
|---|---|---|---|---|---|
| | | Lime | Slag | Hemp | Water |
| 50/50 | R50<br>C50<br>M50<br>F50 | 13.40 | 3.35 | 16.75 | 67.00 |
| 40/60 | R60<br>C60<br>M60<br>F60 | 10.00 | 2.50 | 18.75 | 68.75 |
| **30/70 | C70<br>M70<br>F70 | 7.05 | 1.77 | 20.58 | 70.60 |

* R-received; C-coarse; M-medium; F-fine.
** It was impossible to create a robust 30/70 sample with the shiv received from the manufacturer.

achieved. In contrast, samples tested for compressive strength were tested directly after removal from the curing chamber. Previous studies reported that the direction of casting and compaction affect the thermal and mechanical properties of the hemp-lime composites [4,13,18]. In this study, all mixes were initially cast in a direction perpendicular to heat flow (i.e., vertically). Selected HLC mixes were also cast in a parallel direction (i.e., horizontally) to investigate the effect of casting direction on the thermal properties, and the results were compared with the corresponding mixes cast in the perpendicular direction, as shown in Fig. 2-a.

### 2.5. Experimental tests

#### 2.5.1. Physical and mechanical properties tests

The apparent dry and wet densities were determined due to a significant correlation between the hemp-lime density and its mechanical and hygrothermal properties. Three cubic samples of each mix were used to determine the apparent densities. Given the absence of specific standards governing the measurement and calculation of compressive strength in hemp-lime composites, protocols outlined in BS EN 12390-1 [29] and BS EN 826:2013 [30], devised for concrete and thermal insulation materials in building applications were adhered to for the preparation, testing of samples, and determination of compressive strength [31]. The compressive strength was determined as an average value of six samples for each mix and tested at 30 days using a hydraulic press machine MTS 103. The load was applied in a displacement control manner at a rate of 2 mm/min, and the failure mode was determined when the load-displacement curve reached the maximum value [28]. Fig. 3 illustrates the compressive strength testing setup.

#### 2.5.2. Thermal conductivity

This test was performed on four samples for each hemp-lime mix using a FOX 304 Heat Flow Meter Apparatus (HFMA) following ASTM C518 standard [32] for both perpendicular and parallel cast samples. The apparatus was first calibrated using NIST 1450b SRM (Standard Reference Material of the National Institute of Standards and Technology) to convert the voltage signals into heat flux. Then, the test is conducted using Fourier's law of heat conduction by applying a steady one-dimensional heat flux through the sample by setting a different but constant temperature for the upper and lower plates [28]. For all samples, the thermal conductivity was determined in oven-dry conditions at an average temperature of 12.5 °C where the hot plate was 25 °C

**Fig. 3.** Compressive strength testing setup.


**Fig. 2.** The molds filled with HLC were placed on the vibration table (a) to produce the samples and the test ball method (b) [29].

and the cold plate was 0 °C. Additionally, thermal conductivity was determined at different average temperatures (12.5, 22.5, and 32.5 °C) for selected mixtures, including control mixtures (R50 and R60), and the best-performing mixtures for each B/H ratio (F50, F60, and F70). Furthermore, five different mixes (R50, F50, R60, F60, and F70) were cast in a parallel direction to investigate the effect of casting direction on the thermal properties, and the results were compared with the corresponding mixes cast in the perpendicular direction. For all samples, a high thermal resistance material was placed surrounding the sample to fill up the gap between the chamber walls and the samples to ensure heat flowed through the sample in one direction, as shown in Fig. 4.

### 2.5.3. Specific heat capacity

The specific heat capacity of a material is its ability to store thermal energy [33]. The specific heat capacity was indirectly measured by first measuring the volumetric specific heat using LaserComp FOX 304, as a new method was integrated into the software to measure the volumetric specific heat directly. WinTherm32 software records all the readings of the heat HFMA and calculates the time interval between the readings (typically ~1–1.3 seconds). Then, the software calculates the amount of the total heat per unit square absorbed by both the sample and the instrument using Eq. (5):

$$H = \sum \left[ S_U \left( QU_i - QU_{equil} \right) + S_L \left( QL_i - QL_{equil} \right) \right] \tau, \quad (5)$$

Where $S_U$ and $S_L$ are upper and lower calibration factors, $QU_i$ and $QL_i$ are the HMFAs readings, and $QU_{equil}$ and $QL_{equil}$ are the final equilibrium values of the HFMA signals, which are subtracted to eliminate drift of the sum due to edge heat losses (or gains), and $\tau$ is the time interval between the readings. Then, the software calculates volumetric specific heat value as the amount of heat (per unit of square area and degree °C) absorbed by the sample, divided by the sample's thickness as shown in Eq. (6) [34–37]:

$$C_{p\rho} = \left[ H_{total} / (\Delta T - H_{HFMs}) \right] / L, \quad (6)$$

Where $C_{p\rho}$ is the volumetric specific heat, $H_{total}$ is the total heat absorbed, $\Delta T$ is the temperature change, $H_{HFMs}$ is the heat absorbed by the heat flow meter, and $L$ is the sample thickness. Finally, the specific heat capacity was manually calculated using Eq. (7):

$$C_p = C_{p\rho} / \rho, \quad (7)$$

Where $C_p$is the specific heat capacity, and $\rho$ is density.

### 2.5.4. Thermal diffusivity

This property indicates how fast the material temperature would change when subjected to heating or cooling loads, where the higher the thermal diffusivity, the faster the material would heat or cool and vice versa. Therefore, it is imperative to characterize this property, especially when considering the unsteady state of the heat transfer environment [1]. Thermal diffusivity can be determined using Eq. (8).

$$\alpha = k / \left( \rho . C_p \right), \quad (8)$$

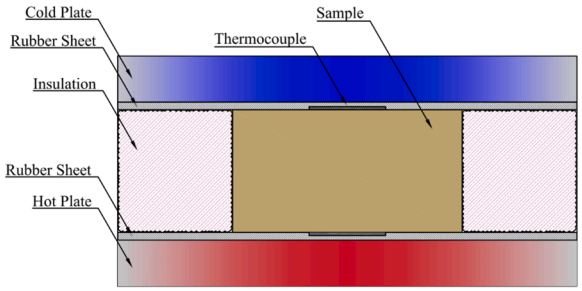


**Fig. 4.** Thermal conductivity setup using FOX 304 Heat Flow Meter.

Where $\alpha$ is the thermal diffusivity and $k$ is the thermal conductivity.

### 2.5.5. Moisture buffering value

Since the hygroscopic behavior of materials subjected to a dynamic humid environment is more realistic than a steady state condition, the Nordtest project introduced an experimental procedure to estimate the moisture buffering behavior of hygroscopic materials using a universal coefficient known as Moisture Buffer Value (MBV) [38]. This coefficient indicates the quantity of water transferred out or in a material per open surface area in a definite time when subjected to varying humidity loading conditions. Under Nordtest, the tested material is subjected to at least three consecutive humidity cycles. The MBV is determined when the test satisfies two conditions: (1) in the last three cycles, the mass difference should be less than 5 %, and (2) within the same cycle, the mass difference in loss or gain should be less than 5 %. Following the Nordtest procedure, four samples of each mix were tested. All sample sides except one (160 mm×160 mm) were sealed. The samples were then placed in an environmental chamber and exposed to a dynamic humidity cycle of 24 hours between high (75 %) and low humidity levels (33 %) for 8 and 16 hours, respectively, at 23±1 °C.

The environmental chambers were built using sealed plastic containers with dimensions of (37.4 ×47.6 ×60.3 cm) and saturated salt solutions to produce 33 % and 75 % relative humidities (RH). ASTM E104–20a standard was followed to produce the humidity levels where 33 % RH was produced by mixing magnesium chloride ($MgCl_2$) with distilled water at a 10:1 wt ratio, while 75 % RH was produced by mixing sodium chloride (NaCl) with distilled water at 2:1 wt ratio [39]. Two humidity sensors were positioned at the top and bottom of each chamber to continuously monitor the humidity levels and ensure the required RH levels and uniform humidity. According to recent research, air velocity can significantly impact the MBV, especially regarding bio-based materials, which can exhibit an increase in MBV by about 150 % when airspeed is increased from 0.108 m/s to 1.91 m/s [40]. In this respect, it is essential to mention that environmental chambers employed in this study use the passive method (i.e., saturated salt solutions) to provide the required moisture conditions while minimizing air movement, unlike conventional climate-controlled environmental chambers with fans or blowers to circulate air within the chamber. The environmental chambers were kept sealed during the test, except when taking weight measurements, and also placed in a climate-controlled lab environment with consistent conditions, including an ambient temperature of 20 ℃ (±1℃), relative humidity of 45 % (±5 %), and air velocity of 0.2 m/s (±0.05 m/s), to minimize further the air movement caused by natural convection due to the variations in ambient conditions. Fig. 5 illustrates the samples and climate chamber. When the test conditions were satisfied, the MBV for each sample was determined using Eq. (9).

$$MBV = \Delta m / (A . \Delta RH), \quad (9)$$

Where $MBV$ is the moisture buffer value, $\Delta m$ is the moisture uptake/

**Fig. 5.** Test assembly and setup of hemp-lime samples in a climate chamber for MBV testing.

release during the cycle, $A$ is the sample exposed area, and $\Delta RH$ is the difference between the highest and the lowest relative humidity.

## 3. Results and discussion

### 3.1. Dry density

Table 4 summarizes the descriptive statistics of dry densities of the hemp-lime samples created using three B/H ratios (1:1, 1:1.5, and 1:2.4) and three hemp shiv particle sizes (received - R, coarse - C, medium - M, and fine - F). Results show a low variability between the dry densities for all B/H ratio categories and sizes of hemp shiv particles. In this regard, all samples' coefficient of variation (CV) is between 0.16 % and 2.36 %. The samples with the F-shiv type exhibited the lowest variability, averaging a CV of 0.56 %. The hemp-lime samples with the highest targeted density of 200 kg/m$^3$ and B/H ratio of 1:1 exhibited the highest variability, averaging 1.84 kg/m$^3$. The consistency achieved in dry densities shows the efficiency of the applied production method, potentially leading to a consistent, repeatable, and reliable mechanical and hygrothermal performance of hemp-lime composites.

Fig. 6 compares the variation in dry density of the samples produced in this study against the previous research that focused on similar densities. The vibrated hemp-lime samples exhibited superior dry density consistency within the targeted weight categories. For example, when using manual tamping as a compaction method to achieve the required density [28], a variation of 17.83 kg/m$^3$ was introduced. Moreover, when machine press compaction and projection process were used [4, 41] to produce hemp-lime samples, a significant variation in densities was produced with a CV of around 16 %. Variations in density were reported within the same sample types where an axial gradient of compactness is observed inside the specimen. Specifically, the density of material near the piston (upper part of the cylinders) was higher than that of material in the lower part. Similar density fluctuations were also noted in the projection process [4,41]. Having such high variation can cause a significant impact on the mechanical and thermal properties as they are both heavily dependent on the density.

### 3.2. Compressive strength

When examining low-strength construction materials such as hemp-lime composites, it is essential to understand the insights gained from testing the material's compressive strength, especially in non-structural applications. While not intended for load-bearing, compressive strength can be a useful measure of relative performance or quality between similar materials. Hence, compressive strength may indicate how well the material can fulfill its intended purpose within its specific environment, considering aspects like durability, constructability in handling, transporting, and installing, and compatibility with other components in the construction assembly. Fig. 7 depicts the hemp-lime samples' two distinct mechanical failure behaviors under continuously applied compressive load. Samples with received shiv behaved as bilinear materials, whereby the curve could be divided into two distinct regions. The first linear phase occurs when the binder fails, and initial cracks propagate. The second linear phase represents significant deformation with less stress development increase than the first. In this phase, the cracking noises became louder, indicating the collapse of the hemp particles, providing additional strength by increasing the contact between those particles. In contrast, hemp-lime samples made of hemp shiv powder exhibited collapse similar to a shear failure, regardless of the particle size. Three different regions can be observed in the stress-strain response: the ascending portion, the peak point or the maximum compressive stress point where the behavior is no longer linear, and finally, the descending portion, where the curve shows a descending trend after reaching maximum stress.

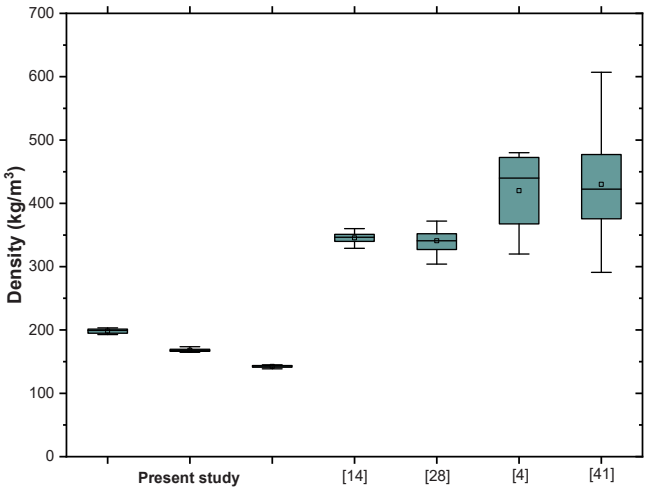


**Fig. 6.** Density variation comparison with other studies.

The stress-strain curve for all samples shows a significant ability of the material to deform under loading before total failure, registering a high level of strains in the range of 0.087–0.26 mm/mm. This behavior could make the hemp-lime composite resilient in earthquake regions as it sustains high deformation before failure. Similar findings were also confirmed by previous literature [13].

As shown in Table 5, the prepared hemp-lime samples displayed satisfactory mechanical performance for such low densities when compared with faced rigid thermal insulation boards [42]. Thus, the average compressive strength ranged between 0.033 MPa and 0.11 MPa. Similar to the findings of other studies [18,41], the compressive strength is directly proportional to dry density and inversely proportional to the increase in hemp shiv share. In this respect, samples with B/H ratios 1:1 producing 200 kg/m$^3$ density exhibit the highest compressive strength value. A 35 % and 45 % reduction in the compressive strength was recorded when the density reduced from 200 kg/m$^3$ to 170 kg/m$^3$ and 140 kg/m$^3$, respectively. The results also show the production method's effectiveness in reducing the variability between the mechanical behavior of hemp-lime composites. The C-type shiv exhibited the lowest variation in compressive strength, with a CV ranging between 4.24 % and 8.94 %. The findings also show a 32–36 % reduction in compressive strength in the 200 kg/m$^3$ and 170 density groups when received particles were replaced with ground particles. The behavior observed is consistent with the findings of [13,15], which reported decreases in strength of 21.6 % and 34.4 % when larger hemp shivs were used instead of smaller ones.

In contrast, [14] found that using larger shivs resulted in a 47.5 % decrease in compressive strength compared to smaller shivs. The

**Table 4**
Descriptive statistics of samples' dry densities.

| Mix ID | Target density (kg/m$^3$) | Dry density (kg/m$^3$) | | | |
|---|---|---|---|---|---|
| | | Mean | Maximum | Minimum | Coefficient of variation % |
| R50 | 200 | 193.30 | 193.90 | 192.72 | 0.31 |
| C50 | | 200.75 | 202.49 | 198.97 | 0.88 |
| M50 | | 199.80 | 203.27 | 196.20 | 1.77 |
| F50 | | 200.12 | 201.80 | 199.10 | 0.73 |
| R60 | 170 | 166.02 | 167.73 | 164.80 | 0.92 |
| C60 | | 166.89 | 167.18 | 166.70 | 0.16 |
| M60 | | 168.97 | 173.50 | 166.02 | 2.36 |
| F60 | | 169.87 | 170.51 | 169.24 | 0.37 |
| *C70 | 140 | 140.67 | 143.80 | 138.53 | 1.97 |
| M70 | | 142.38 | 143.12 | 141.15 | 0.75 |
| F70 | | 143.92 | 144.98 | 142.89 | 0.59 |

* It was impossible to create a robust 30/70 sample with the shiv received from the manufacturer.

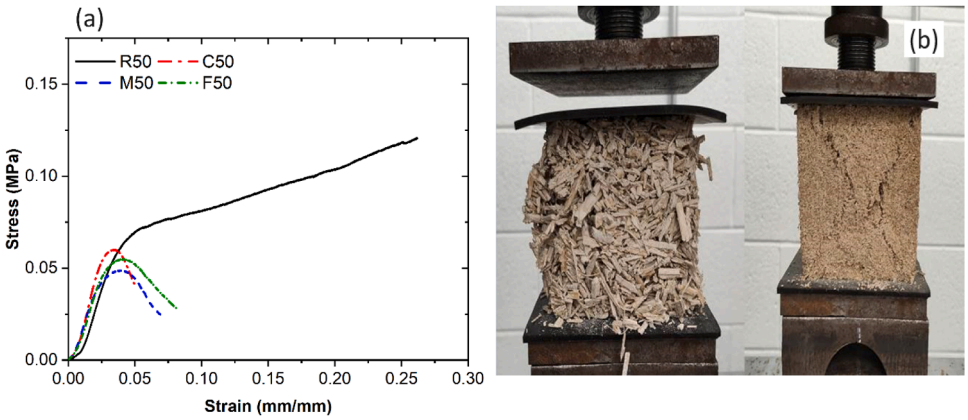


**Fig. 7.** Typical stress-strain curve for hemp-lime samples (a); Compressive Strength test, hemp-lime cubes after crushing (b).

**Table 5**
Descriptive statistics of samples' compressive strength.

| Mix ID | Density category (kg/m$^3$) | Compressive Strength (MPa) | | Young's modulus (MPa) | |
|---|---|---|---|---|---|
| | | Mean | Coefficient of variation % | Mean | Coefficient of variation % |
| R50 | 200 | 0.111 | 9.91 | 3.96 | 7.38 |
| C50 | | 0.070 | 5.71 | 3.76 | 5.01 |
| M50 | | 0.070 | 7.86 | 3.27 | 5.43 |
| F50 | | 0.071 | 19.72 | 3.22 | 13.82 |
| R60 | 170 | 0.072 | 13.89 | 2.81 | 8.63 |
| A60 | | 0.047 | 8.94 | 2.74 | 7.62 |
| M60 | | 0.045 | 19.56 | 2.93 | 11.89 |
| F60 | | 0.049 | 10.00 | 2.61 | 6.31 |
| *C70 | 140 | 0.033 | 4.24 | 2.09 | 3.28 |
| M70 | | 0.036 | 24.44 | 1.91 | 16.32 |
| F70 | | 0.042 | 14.29 | 1.82 | 7.54 |

discrepancy may be attributed to the average densities: large shivs had an average density of 1040 kg/m$^3$, while small shivs had an average density of 1150 kg/m$^3$, a 10.57 % difference. Such a variation in density can significantly influence compressive strength, as shown in this study, where a 15 % reduction in density from 200 kg/m$^3$ to 170 kg/m$^3$ led to about a 40 % decrease in average compressive strength.

Table 5 also presents approximate Young's modulus values calculated using the displacement values of the actuator, as it was challenging to mount the compressometer directly to the sample. As shown in Table 5, the average modulus of elasticity ranged between approximately 1.82 and 3.96 MPa. Results show a direct relationship between HLC dry density and Young's modulus. In this respect, a 15 % reduction in density from 200 kg/m$^3$ to 170 kg/m$^3$ led to an approximately 22 % decrease in average Young's modulus. Similarly, a further decrease in density from 170 kg/m$^3$ to 140 kg/m$^3$ resulted in around 30 % reduction in average Young's modulus. Findings also show a negative correlation between Young's modulus and hemp shiv particle size.

Fig. 8 compares the relationship between the density and the compressive strength results obtained from this study and the previous studies that used a hydrated lime-based binder [13,14,18, and 28]. As documented in prior studies, the compressive strength and density are directly and inversely proportional [15,28]. Therefore, Fig. 8 illustrates that when the results of this study are extrapolated to the available range of densities, they align with the findings reported in the previous literature. Bryziki [13] and Williams [18] have reported higher compressive strength values than other studies, which can be explained using a B/H ratio of 2:1 and 2.25:1, respectively. As reported by previous literature, an increase in binder content in the formulation leads to an almost linear increase in compressive strength [10].

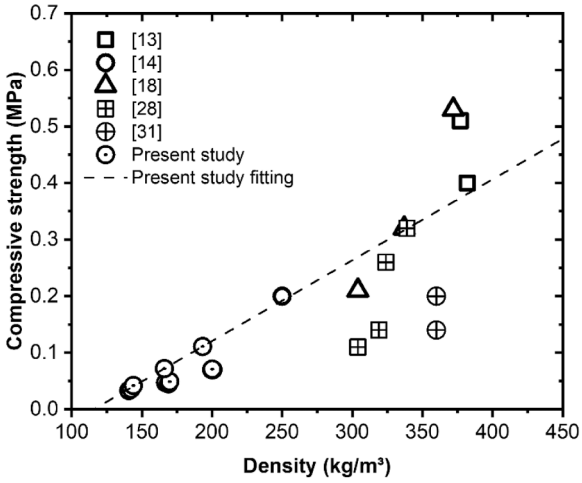


**Fig. 8.** Comparison of density and compressive strength with the previous literature.

### 3.3. Thermal properties

#### 3.3.1. Thermal conductivity

Table 6 summarizes the results of thermal conductivity measurements. As expected, thermal conductivity is positively linearly correlated with the dry density of the hemp-lime composites [28]. Hence, samples with the lowest dry density (140 kg/m$^3$) had the lowest thermal conductivity, ranging from 0.054 to 0.056 W/m K, followed by

**Table 6**
Descriptive statistics of samples' thermal conductivity.

| Mix ID | Mean dry density (kg/m$^3$) | Thermal conductivity (W/m K) | | | |
|---|---|---|---|---|---|
| | | Mean | Maximum | Minimum | Coefficient of variation % |
| R50 | 193 | 0.0667 | 0.0713 | 0.0612 | 6.66 |
| C50 | 201 | 0.0638 | 0.0701 | 0.0589 | 8.76 |
| M50 | 200 | 0.0616 | 0.0674 | 0.0581 | 6.70 |
| F50 | 200 | 0.0605 | 0.0625 | 0.0572 | 3.87 |
| R60 | 166 | 0.0617 | 0.0683 | 0.0573 | 7.75 |
| C60 | 167 | 0.0587 | 0.0622 | 0.0562 | 4.96 |
| M60 | 169 | 0.0579 | 0.0621 | 0.0555 | 5.11 |
| F60 | 170 | 0.0564 | 0.0597 | 0.0532 | 4.63 |
| *C70 | 141 | 0.0559 | 0.0593 | 0.0538 | 6.05 |
| M70 | 142 | 0.0545 | 0.0589 | 0.0522 | 5.71 |
| F70 | 144 | 0.0535 | 0.0572 | 0.0502 | 5.40 |

* It was impossible to create a robust 30/70 sample with the shiv received from the manufacturer.

170 kg/m$^3$ samples with 0.056–0.062 W/m K, and 200 kg/m$^3$ with the highest thermal conductivity ranging from 0.061 to 0.067 W/m K. It can also be observed that samples made of received shiv particles exhibited the highest thermal conductivity values within density category. Furthermore, the hemp-lime samples made with fine hemp particles tend to have the lowest thermal conductivity despite having the highest or as high density within their respective density categories. In this regard, thermal conductivity was reduced by 8.1–10.4 % when using the fine fragments compared to the received. A likely explanation for these findings is a discontinuity in the binder thermal path when using small hemp shiv particles, reducing the overall thermal conductivity of hemp-lime composites. These findings suggest that reducing the hemp shiv particle size benefits the thermal performance of hemp-lime composites.

Table 6 also shows the low variability in the thermal conductivity values across the samples at different densities, achieved using the vibration casting technique. Therefore, the CV of all samples was between 3.87 % and 8.77 %. The samples with the finest particle size exhibited the lowest variability, recording 3.87, 4.63, and 5.6 % for samples with 200, 170, and 140 kg/m$^3$ density, respectively.

Fig. 9 compares the correlation between dry density and thermal conductivity from this research with other studies [4,13,18, and 28]. It can be seen that the thermal conductivity values from this study are 25–65 % lower than those reported in previous studies, and correspondingly, the dry densities are also 28–65 % lower. To facilitate a seamless comparison, the thermal conductivity results from this study have been extrapolated, considering the nearly linear relationship between density and thermal conductivity [28], to match the average densities reported in the other studies presented in Fig. 9. The extrapolated thermal conductivity values were 0.0775, 0.0828, 0.0778, and 0.07425 W/m K, which correspond to the average densities of (335, 380, 340, and 310 kg/m$^3$) reported in [4, 13, 18, and 28], in that order. The extrapolated values from this study are 18.82 %, 11.22 %, and 19.16 % lower in thermal conductivity compared to the values documented in [13,18,28], respectively. The extrapolated thermal conductivities are only 1.35 % higher than those reported by [4]. These findings suggest that a decrease in hemp particle sizes reduces hemp-lime composites' thermal conductivity, thus improving the material's thermal performance even at higher densities.

### 3.3.2. Thermal conductivity as a function of temperature

Thermal conductivity was assessed at three distinct temperature levels (12.5°C, 22.5°C, and 32.5°C) to evaluate the performance of hemp-lime composites across various climate zones. The study included selected hemp-lime mixes (F50, F60, and F70) with dry densities of 200 kg/m$^3$, 170 kg/m$^3$, and 140 kg/m$^3$, respectively. These mixes represent the optimal thermal performance within their respective groups, exhibiting the lowest thermal conductivity. Fig. 10 shows a nearly linear increase in thermal conductivity across all the samples, ranging from 6.6 % to 9.8 %, with a rise in testing temperature from 12.5 °C to 32.5 °C. These results echo the findings from previous studies that reported an increase in conductivity of 8.9–10.78 % when the temperature increased from 10 °C to 30°C [43]. This behavior is attributed to the increased thermal conductivity of air entrapped in the sample from 0.0253 W/m K at 12.5°C to 0.0268 W/m K at 32.5°C [44].

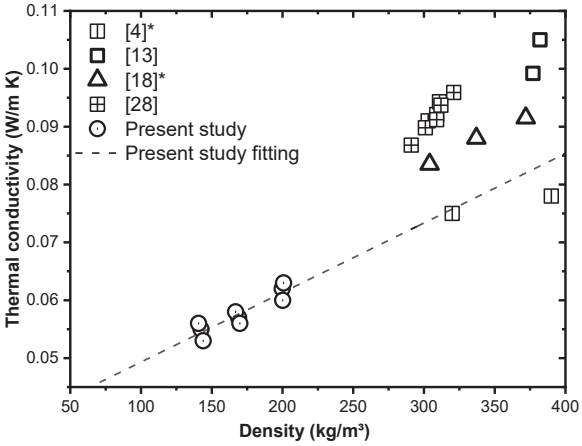


**Fig. 9.** Comparing thermal conductivity results with other studies.

### 3.3.3. Anisotropy of thermal conductivity

The effect of hemp shiv orientation due to compaction via vibration on thermal conductivity is also investigated due to the inherently anisotropic nature of hemp particles, where thermal conductivity in the direction parallel to the capillaries is higher than in the transversal direction [4]. In this respect, EN ISO 10456 standard [45] reports two values with a significant difference reaching up to 27 % for the thermal conductivity of wood particles when heat flows along the material fibers versus when heat transfers across the fibers. Previous studies showed a significant effect of the compaction direction of hemp-lime composites on their thermal conductivity coefficients. For example, Brzyski [16] has reported a 12 % and 16 % difference in thermal conductivity in the parallel and perpendicular direction for short (2.74 mm) and long (8.40 mm) hemp shivs, respectively. Williams [18] reported that the average thermal conductivity for perpendicularly tested samples was 16 % higher than that of parallel-tested samples. Pierre [46] has also reported a 33 % directional difference in thermal conductivity, similar to what was reported in [47,48].

In contrast, as presented in Fig. 11, this study significantly improved the directional difference in thermal conductivity to only 1.2–2.75 % when using fine hemp fragments and approximately 6.8 % when using R-shiv. The results confirm the previously reported trend as the smaller the hemp shiv, the lower the difference [16]. It also shows the significant effect of using compaction via vibration, leading to a consistent performance of the hemp composite. The perpendicular thermal conductivity results also have a linear relationship with the dry density, as the lower the density, the lower the conductivity.

### 3.3.4. Specific heat capacity and thermal diffusivity

As shown in Table 7, the specific heat capacity of the hemp-lime samples ranged from 672 to 957 J/kg K. As expected, mixes with higher dry density and binder content had higher specific heat capacity, meaning more heat energy is needed to raise their temperature. For instance, 200 kg/m$^3$ samples had around 28 % higher average specific heat capacity than 140 kg/m$^3$ samples and approximately 15 % higher than 170 kg/m$^3$ samples. The findings also show no tangible effect of the

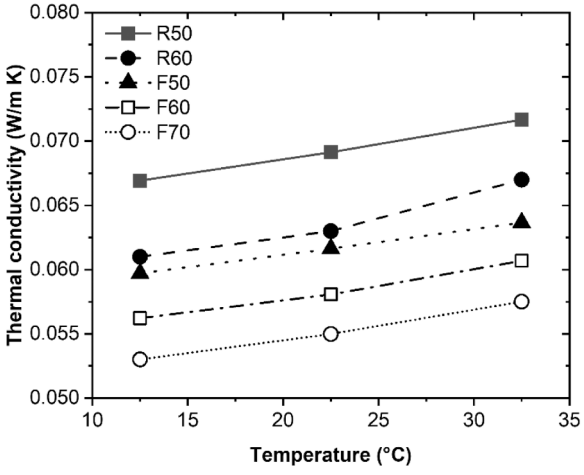


**Fig. 10.** Thermal conductivity of different hemp-lime mixes at different testing temperatures.

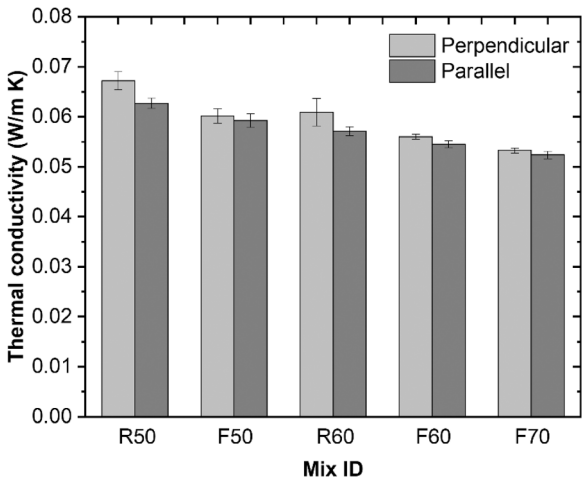


**Fig. 11.** Thermal conductivity for different testing directions.

**Table 7**
Average specific heat capacity and thermal diffusivity.

| Mix ID | Dry density category (kg/m$^3$) | Ave. Specific heat capacity (J/kg K) | Coefficient of variation % | Ave. Thermal diffusivity (m$^2$/s) x10$^{-6}$ | Coefficient of variation % |
|---|---|---|---|---|---|
| R50 | 200 | 942 | 4.21 | 0.368 | 3.23 |
| C50 | | 931 | 6.79 | 0.337 | 5.75 |
| M50 | | 957 | 3.01 | 0.324 | 4.39 |
| F50 | | 933 | 2.26 | 0.321 | 3.56 |
| R60 | 170 | 803 | 6.43 | 0.458 | 6.93 |
| C60 | | 798 | 5.27 | 0.436 | 4.22 |
| M60 | | 782 | 2.68 | 0.431 | 3.71 |
| F60 | | 811 | 4.11 | 0.406 | 5.03 |
| *C70 | 140 | 681 | 5.79 | 0.585 | 4.68 |
| M70 | | 672 | 4.38 | 0.575 | 3.41 |
| F70 | | 689 | 4.17 | 0.534 | 3.79 |

* It was impossible to create a robust 30/70 sample with the shiv received from the manufacturer

hemp shiv size on the specific heat values, concluding that hemp composites are more susceptible to density and binder ratio than hemp shiv size [13]. The results also confirm the general trend of the linear relationship between hemp-lime's density and specific heat capacity. Previous studies echoed these findings. For example, in [6], two different mixes, A (394.8 kg/m$^3$) and B (298.1 kg/m$^3$), with binder-to-hemp mass ratios of 1.8 and 1.13, respectively, have been investigated. The study found that mix B, which had a higher hemp content and lower dry density, exhibited an average specific heat capacity of 333 J/kg K, approximately 13.5 % lower than mix A, which had a lower hemp content and higher dry density, with a specific heat capacity of 385 J/kg K.

Thermal diffusivity measures a material's ability to conduct heat relative to its ability to store thermal energy, quantifying the rate at which temperature changes propagate through the material over time [6]. Building materials with low thermal diffusivity reduce heat exchange with their surroundings, leading to improved energy efficiency and thermal comfort for occupants [28]. Thermal diffusivity of all samples ranged between 0.321 (m$^2$/s) x10$^{-6}$ and 0.585 (m$^2$/s) x10$^{-6}$, with averages of 0.338, 0.433, and 0.565 (m$^2$/s) x10$^{-6}$ for samples with 200, 170, and 140 kg/m$^3$ density categories, respectively. The densest (200 kg/m$^3$) samples exhibited around 40 % lower thermal diffusivity than the lightest (140 kg/m$^3$) and approximately 22 % lower than the 170 kg/m$^3$ hemp-lime samples. These findings were expected considering the interdependency between thermal diffusivity, thermal conductivity, and density (see Eq. 8). Furthermore, the high thermal diffusivity of air of 18.69 (m$^2$/s) x10$^{-6}$ [49] increased the thermal diffusivity of low-density samples. These findings echo previous studies [6,28,50,51]. The results also show a lower diffusivity value for samples with smaller hemp fragments. For example, F-type shiv particles were around 13 % and 11 % lower than R-type shiv for 200 and 170 kg/m$^3$ density samples. Such reduction could be attributed to filling the air gap between constituents when small hemp shiv particles were used.

### 3.4. Moisture buffer value

Moisture buffering ability plays a vital role in regulating the fluctuation in humidity in internal spaces. As illustrated in Fig. 12, all the samples showed an excellent moisture buffering capacity [38], as the average moisture buffer value (MBV) ranged between 2.06 g/m$^2$ RH and 2.53 g/m$^2$ RH. The results show a negative correlation between dry density and MBV of hemp-lime composites. In this regard, average MBV values of 140, 170, and 200 kg/m$^3$ samples were 2.47, 2.28, and 2.12 g/m$^2$ RH, respectively. A similar trend is confirmed by previous literature, as a high hemp ratio in the composite produces lower density and higher permeability, leading to a high moisture transfer and storage of the material [52]. Therefore, an increase in the hemp ratio in the hemp composite results in an increase in the moisture capacity, which causes an increase in the MBV. The results also showed an improvement in the MBV when using a smaller hemp shiv size.

Additionally, Fig. 13 shows the mass change percentage concerning the original sample mass for the F-type shiv when exposed to the humidity cycles during the MBV test. The mass change was determined per the exposed surface area and was measured every four hours. It can be seen that regardless of the B/H ratio, all samples showed similar mass change behavior. The mass change profile consists of two phases: the mass phase increases when the humidity level is 75 %, while the decreasing phase occurs at a 33 % humidity level. For both phases, the initial hours 0–8 hours record the highest rate of mass change, and then the change rate decreases with time. It can also be seen that the higher the hemp shiv ratio, the higher the mass change gain; thus, F70 samples have the highest mass gain. This behavior is attributed to the high absorption capacity of the hemp compared to the binder.

Fig. 14 compares the uptake moisture buffering capacity at oven-dry as an initial condition for the three groups used in the study with B/H ratios 1:1, 1:1.5, and 1:2.4. It can be seen that the moisture buffering capacity starts at high values ranging between 2.5 g/m$^2$ RH and 3.6 g/m$^2$ RH then it starts decreasing until reaching steady-state by the third cycle. This increase is attributed to the high absorption capacity of the hemp-lime samples when they have low moisture content, whereas higher initial moisture content leads to lower absorption. Fig. 14 shows a distinct behavior for the R-type hemp-lime samples where the decrease

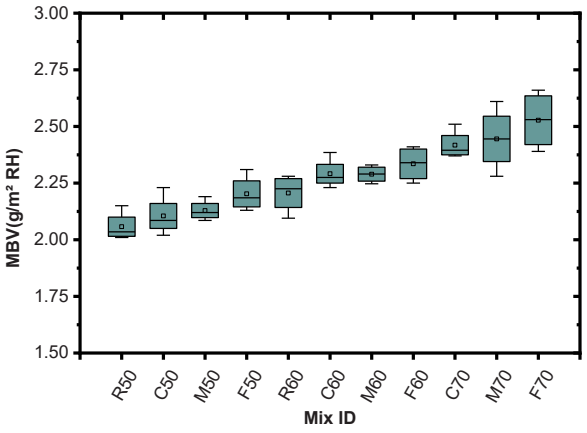


**Fig. 12.** MBV values of the hemp-lime samples using the NORDTEST procedure.

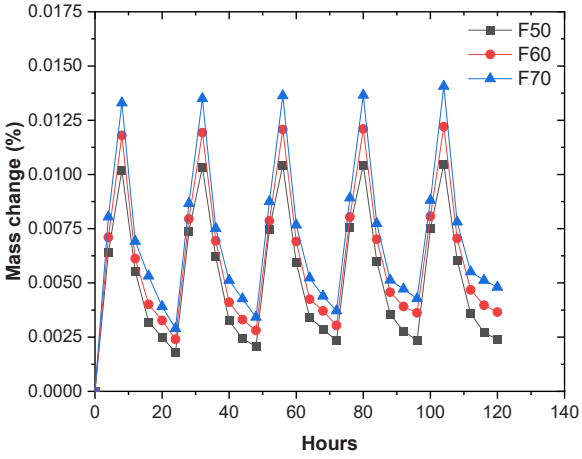


**Fig. 13.** Mass change of the hemp-lime samples when subjected to varying relative humidity at room temperature.

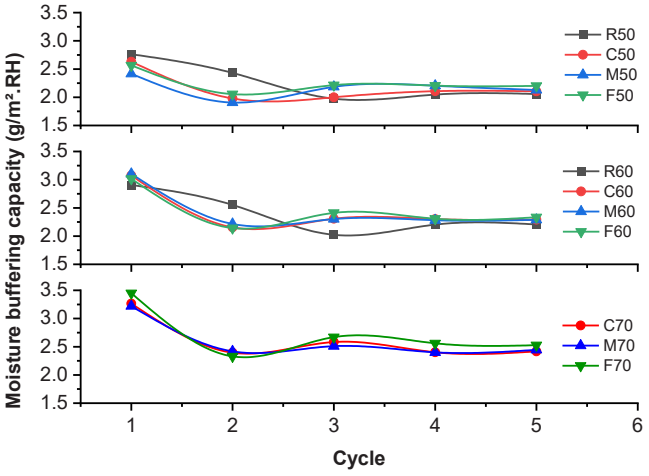


**Fig. 14.** Moisture buffering capacity with cycles.

in the absorption from the first cycle takes longer than that of other types as they have a lower surface area. It can be concluded that hemp-lime composites with lower particle size can achieve moisture stability faster, leading to better moisture control performance.

## 4. Conclusions, limitations, and future work

Hemp-lime composites increasingly capture the spotlight in the construction sector due to their remarkable sustainability, minimal environmental impact, and impressive hygrothermal properties, making them a compelling choice for environmentally-conscious builders seeking durable and eco-friendly construction materials. However, the widespread adoption of hemp-lime composites has encountered obstacles due to significant variations in formulation and manufacturing techniques, leading to inconsistent mechanical properties and hygrothermal performance. This study addresses these limitations by introducing a novel methodology to enhance the homogeneity and uniformity of hemp-lime composites, rendering their performance as predictable, reproducible, and consistent as traditional insulation materials. The new approach holistically addressed the variability of hemp-lime composites through two steps: (1) reducing the hemp shiv particle sizes from received of 4.52 mm to 1.33, 0.96, and 0.72 mm for coarse, medium, and fine particle sizes, respectively, (2) using vibration as a compaction method to produce uniform samples. The hygrothermal and mechanical characterization showed improved insulating and moisture buffer properties of samples with reduced particle sizes compared to the control sample made of the received shiv and similar studies. The principal conclusions drawn from this study and limitations that guide future research directions can be summarized as follows:

- The experimental findings highlight the significance of reducing and standardizing the shiv particle size, resulting in a notable enhancement in material consistency and a reduction in variations across mechanical and hygrothermal properties among samples of the same targeted density. Furthermore, this reduction in particle size was pivotal in achieving a 70 % weight share of the bio-based component in the hemp-lime mix design. Subsequent research endeavors should delve into the effects of particle size reduction and augmented hemp shive content on properties such as fire resistance, freeze-thaw behavior, biological degradation, and durability.
- Employing vibration as a compaction method significantly enhanced the consistency and repeatability of the produced densities, showcasing a less than 3.5 % variation. Hence, the density disparities between the initial and fine hemp fragments were also negligible. Given the substantial influence of density on the hygrothermal and mechanical properties of hemp-lime composites, attaining such uniformity facilitates the material's adoption in the construction industry and large-scale applications. Consequently, future endeavors should prioritize optimizing hemp-lime composite mix designs tailored for various applications in building envelopes (walls, floors, ceilings), envelope component designs (blocks, panels), and installation methods (sprayed-in, precast).
- Although the hemp-lime composite may not match the structural capabilities of other load-bearing construction materials, it does fall within the compressive strength range of faced rigid insulation materials ranging between 0.11 and 0.965 MPa. Future research could explore alternative binder mix designs, incorporating pozzolans such as metakaolin, silica fume, and fly ash. In addition to enhancing mechanical properties, these pozzolans have the potential to positively influence the long-term alkalinity and durability of hemp-lime composites. Subsequent research should further optimize the binder mix design and distribution between hydrated lime and added pozzolans. Additionally, adjustments to the binder-to-hemp ratio could be made to meet specific mechanical requirements.
- The received shiv exhibited a 60 % increase in strength compared to fine fragments and demonstrated a distinct failure pattern characterized by bi-linear behavior, contrasting with the shear failure mode observed in fine fragments. Subsequent investigations should prioritize optimizing the particle size distribution by exploring various ratios of coarse and fine particles, aiming to enhance compressive strength while minimizing thermal conductivity.
- Hemp-lime samples containing fine hemp fragments displayed an approximate 13 % decrease in thermal conductivity compared to those with received shivs. This observation suggests that thermal conductivity is influenced by shiv size since uniformly reducing hemp particle size diminished areas containing predominant binder content with an inherently higher thermal conductivity than hemp shivs. Future research should focus on optimizing the smallest particle size of hemp shivs and determining its threshold to prevent unnecessary expenditure of energy and resources on grinding and preprocessing. Furthermore, developing a detailed and validated finite element or finite volume thermal model could provide further insight and explanation of the experimental results.
- The results demonstrate a noteworthy enhancement in the directional difference of thermal conductivity, reduced to less than 3 % when employing fine hemp fragments. These findings suggest that the proposed hemp shiv reduction approach could facilitate the creation of building envelope components with uniform thermal properties. In addition, it could enable the development of building envelopes with predictable thermal performance, accommodating

various installation methods such as projection, precast, and printing.

- Hemp-lime mixes with a higher hemp-to-binder ratio demonstrate improved moisture control, attributed to hemp's greater moisture storage capacity than the binder mixture. Additionally, reducing the hemp size enhances the moisture buffer value by increasing the exposed surface area to the outside environment. However, further investigation is warranted to confirm this behavior conclusively. Additionally, the impact of air velocity on the variations in moisture buffer values should be investigated.

## Funding

This research was funded by the Natural Sciences and Engineering Research Council (NSERC) Alliance Grant with the number 580866.

## CRediT authorship contribution statement

**Martin Noel:** Writing – review & editing, Supervision, Resources, Project administration, Methodology, Funding acquisition, Conceptualization. **Miroslava Kavgic:** Writing – review & editing, Writing – original draft, Supervision, Resources, Project administration, Methodology, Funding acquisition, Conceptualization. **Osamah Mahmood:** Writing – review & editing, Writing – original draft, Visualization, Validation, Methodology, Investigation, Formal analysis, Data curation, Conceptualization.

## Declaration of Competing Interest

The authors declare that they have no known competing financial interests or personal relationships that could have appeared to influence the work reported in this paper.

## Acknowledgment

The authors would like to acknowledge the in-kind contribution of "Terrafibre," "the Canadian Hemp Trade Alliance, CHTA," and "Lafarge."

## Data Availability

Data will be made available on request.

## References

[1] M. Lawrence, Reducing the environmental impact of construction by using renewable materials, J. Renew. Mater. 3 (3) (2015) 163–174, https://doi.org/10.7569/JRM.2015.634105.
[2] N. Holcroft, A. Shea, Effect of compaction on moisture buffering of hemp-lime insulation, Acad. J. Civ. Eng. 33 (2) (2015) 542–546, https://doi.org/10.26168/icbbm2015.84.
[3] D. Barnat-Hunek, P. Smarzewski, S. Fic, Mechanical and thermal properties of hemp-lime composites, Compos. Theory Pract. 15 (2015) 21–27.
[4] T. Nguyen, V. Picandet, P. Carre, T. Lecompte, S. Amziane, C. Baley, Effect of compaction on mechanical and thermal properties of hemp concrete, Eur. J. Env. Civ. Eng. 14 (2010), https://doi.org/10.3166/EJECE.14.545-560.
[5] Experimental investigation on the influence of immersion/ drying cycles on the hygrothermal and mechanical properties of hemp concrete, Ferhat Benmahiddine a, b, c, Fares Bennai d, Rachid Cherif a, Rafik Belarbi a, b, *, Abdelkader Tahakourt c, Kamilia Abahri e.
[6] Paulien de Bruijn, Peter Johansson, Moisture fixation and thermal properties of lime–hemp concrete, 242,ISSN 0950-0618, Constr. Build. Mater. 47 (2013) 1235, https://doi.org/10.1016/j.conbuildmat.2013.06.006.
[7] V. Nozahic, S. Amziane, Influence of sunflower aggregates surface treatments on physical properties and adhesion with a mineral binder, ISSN 1359-835X, Compos. Part A: Appl. Sci. Manuf. 43 (11) (2012) 1837–1849, https://doi.org/10.1016/j.compositesa.2012.07.011.
[8] V. Nozahic, S. Amziane, G. Torrent, K. Saïdi, H. De Baynast, Design of green concrete made of plant-derived aggregates and a pumice–lime binder, ISSN 0958-9465, Cem. Concr. Compos. 34 (2) (2012) 231–241, https://doi.org/10.1016/j.cemconcomp.2011.09.002.
[9] M. Sinka, L. Radina, G. Sahmenko, A. Korjakins, D. Bajare, Enhancement of Lime-Hemp concrete properties using different manufacturing technologies, Acad. J. Civ. Eng. 33 (2) (2015) 301–308, https://doi.org/10.26168/icbbm2015.46.
[10] M.P. Sáez-Pérez, M. Brümmer, J.A. Durán-Suárez, A review of the factors affecting the properties and performance of hemp aggregate concretes, ISSN 2352-7102, J. Build. Eng. 31 (2020) 101323, https://doi.org/10.1016/j.jobe.2020.101323.
[11] F. Collet, J. Chamoin, S. Pretot, C. Lanos, Comparison of the hygric behaviour of three hemp concretes, Energy Build. 62 (2013) 294–303, https://doi.org/10.1016/j.enbuild.2013.03.010.
[12] C. Niyigena, S. Amziane, A. Chateauneuf, L. Arnaud, L. Bessette, F. Collet, C. Lanos, G. Escadeillas, M. Lawrence, C. Magniont, S. Marceau, S. Pavia, U. Peter, V. Picandet, M. Sonebi, P. Walker, Variability of the mechanical properties of hemp concrete, Mater. Today Commun. 7 (2016) 122–133, https://doi.org/10.1016/j.mtcomm.2016.03.003.
[13] P. Brzyski, M. Gładecki, M. Rumińska, K. Pietrak, M. Kubiś, P. Łapka, Influence of Hemp shives size on hygro-thermal and mechanical properties of a hemp-lime composite, Materials 13 (23) (2020) 5383, https://doi.org/10.3390/ma13235383.
[14] N. Stevulova, L. Kidalova, J. Junak, J. Cigasova, E. Terpakova, Effect of hemp shive sizes on mechanical properties of lightweight fibrous composites, Procedia Eng. 42 (2012) 496–500, https://doi.org/10.1016/j.proeng.2012.07.441.
[15] L. Arnaud, E. Gourlay, Experimental study of parameters influencing mechanical properties of hemp concretes, Constr. Build. Mater. 28 (1) (2012) 50–56, https://doi.org/10.1016/j.conbuildmat.2011.07.052.
[16] P. Brzyski, P. Gleń, M. Gładecki, M. Rumińska, Z. Suchorab, G. Łagód, Influence of the direction of mixture compaction on the selected properties of a hemp-lime composite, Materials 14 (2021) 4629, https://doi.org/10.3390/ma14164629.
[17] J. Williams, M. Lawrence, P. Walker, A method for the assessment of the internal structure of bio-aggregate concretes, Constr. Build. Mater. 116 (2016) 45–51, https://doi.org/10.1016/j.conbuildmat.2016.04.088.
[18] J. Williams, M. Lawrence, P. Walker, The influence of the casting process on the internal structure and physical properties of Hemp-Lime, Mater. Struct. 50 (2) (2016) 108, https://doi.org/10.1617/s11527-016-0976-4.
[19] C.ésar Niyigena, Sofiane Amziane, Alaa Chateauneuf, Multicriteria analysis demonstrating the impact of shiv on the properties of hemp concrete, ISSN 0950-0618, Constr. Build. Mater. Volume 160 (2018) 211–222, https://doi.org/10.1016/j.conbuildmat.2017.11.026.
[20] Amziane, S., F. Collet, M. Lawrence, C. Magniont, and V. Picandet. "Round robin test for hemp shiv characterization." Bio-aggregates based building materials: State of the art report of the RILEM Technical Committee.
[21] Sofiane Amziane, Collet Florence (Eds.), Bio-aggregates based building materials: state-of-the-art report of the RILEM Technical Committee 236-BBM, Springer, 2017. Vol. 23.
[22] V. Nozahic (2012). Vers une nouvellement démarche de conception des bétons de végétaux lignocellulosiques basée sur la compréhension et l'amélioration de l'interface liant/ végétal application à des granulats de chènevotte et tige de tournesol associés à un liant ponce/ chaux". Thèse de doctorant. Université Blaise Pascal.
[23] C. Igathinathane, L.O. Pordesimo, E.P. Columbus, W.D. Batchelor, S. Sokhansanj, Sieveless particle size distribution analysis of particulate materials through computer vision, Comput. Electron. Agric. Vol. 66 (2009) 147–158.
[24] ASTM C207-06. Standard Specification for Hydrated Lime for Masonry Purposes, ASTM International, West Conshohocken, PA, USA, 2006.
[25] ASTM C989/C989M-18a, Standard Specification for Slag Cement for Use in Concrete and Mortars, ASTM International, West Conshohocken, PA, USA, 2018.
[26] R. Walker, S. Pavía, Physical properties and reactivity of pozzolans, and their influence on the properties of lime–pozzolan pastes. Mater. Struct. 44 (2011) 1139–1150.
[27] Nima Asghari, Ali M. Memari, State of the art review of attributes and mechanical properties of hempcrete, Biomass 4 (1) (2024) 65–91, https://doi.org/10.3390/biomass4010004.
[28] Y. Abdellatef, M.A. Khan, A. Khan, M.I. Alam, M. Kavgic, Mechanical, Thermal, and moisture buffering properties of novel insulating hemp-lime composite building materials, Materials 13 (21) (2020) 5000, https://doi.org/10.3390/ma13215000.
[29] BS EN 12390-1, British Standard for Testing Hardened Concrete—Part 1: Shape, Dimensions and Other Requirements for Specimens and Moulds, BSI, London, 2000.
[30] British Standards (2013) BS EN 826:2013—thermal insulating products for building applications. Determination of compression behaviour. Wärmedämmstoffe für das Bauwesen. Bestimmung des Verhaltens bei Druckbeanspruchung.
[31] R. Walker, S. Pavia, R. Mitchell, Mechanical properties and durability of hemp-lime concretes, Constr. Build. Mater. 61 (2014) 340–348, https://doi.org/10.1016/j.conbuildmat.2014.02.065.
[32] ASTM C518–17, Standard Test Method for Steady-State Thermal Transmission Properties by Means of the Heat Flow Meter Apparatus, ASTM International, West Conshohocken, PA, USA, 2017.
[33] S. Dubois, A. Evrard, F. Lebeau, Modeling the hygrothermal behavior of biobased construction materials, J. Build. Phys. 38 (2014) 191–213.
[34] Tleoubaev, A., and Brzezinski, A. 2007. "Thermal Diffusivity and Volumetric Specific Heat Measurements Using Heat Flow Meter Instruments" presented at the Thermal Conductivity 29 / Thermal Expansion 17 Conference, June 2007, Birmingham, Alabama. (⟨www.lasercomp.com⟩ "Technical Papers and Publications").
[35] H.S. Carslaw, J.C. Jaeger. Conduction of Heat in Solids, second edition, Oxford at the Clarendon Press, 1959.

[36] D.R. Flynn, R. Gorthala, Earlytime estimation of the thermal resistance of flat specimens – theoretical analysis for pure conduction in a homogeneous material, in: R.S. Graves, R.R. Zarr (Eds.), in: Insulation Materials: Testing and Applications: Third Volume, ASTM STP 1320, American Society for Testing and Materials, 1997 381400.
[37] A.N. Tikhonov, A.A. Samarskii, Equations of Mathematical Physics, Dover Publications, Inc, 1963 515516.
[38] Rode, C.; Peuhkuri, R.H.; Hansen, K.K.; Time, B.; Svennberg, K.; Arfvidsson, J.; Ojanen, T. NORDTEST Project on Moisture Bu_er Value of Materials. In Proceedings of the AIVC 26th Conference: Ventilation in Relation to the Energy Performance of Buildings, Brussels, Belgium, 21–23 September 2005; pp. 47–52.
[39] ASTM E104-20a. Standard Practice for Maintaining Constant Relative Humidity by Means of Aqueous Solutions, ASTM International, West Conshohocken, PA, USA, 2020.
[40] S. Khaled, F. Collet, S. Prétot, M. Bart, Effect of air velocity and initial conditioning on the moisture buffer value of four different building materials, Materials *16* (2023) 3284, https://doi.org/10.3390/ma16083284.
[41] S. Elfordy, F. Lucas, F. Tancret, Y. Scudeller, L. Goudet, Mechanical and thermal properties of lime and hemp concrete ("hempcrete") manufactured by a projection process, ISSN 0950-0618, Constr. Build. Mater. Volume 22 (Issue 10) (2008) 2116–2123, https://doi.org/10.1016/j.conbuildmat.2007.07.016.
[42] ASTM C1289-22a. Standard Specification for Faced Rigid Cellular Polyisocyanurate Thermal Insulation Board, ASTM International, West Conshohocken, PA, USA, 2022.
[43] F. Bennai, N. Issaadi, K. Abahri, et al., Experimental characterization of thermal and hygric properties of hemp concrete with consideration of the material age evolution, Heat. Mass Transf. 54 (2018) 1189–1197, https://doi.org/10.1007/s00231-017-2221-2.
[44] De Witt, (2002). New York (NY) Fundam. Heat. Mass Transf.
[45] European Committee for Standardization, (2007). Building Materials and Products. Hygrothermal Properties. Tabulated Design Values and Procedures for Determining Declared and Design Thermal Values; ISO 10456:2007; European Committee for Standardization: Geneva, Switzerland.
[46] P. Tronet, T. Lecompte, V. Picandet, C. Baley, Study of lime hemp concrete (LHC) – Mix design, casting process and mechanical behaviour, ISSN 0958-9465, Cem. Concr. Compos. 67 (2016) 60–72, https://doi.org/10.1016/j.cemconcomp.2015.12.004.
[47] Amziane S., Nozahic V., Sonebi M. (2015). Design of mechanically enhanced concrete using hemp shiv First international conference on bio-based building materials. Clermont-Ferrand, France.
[48] Dinh T. et al. (2015). Hemp concrete using innovative pozzolanic binder First international conference on bio-based building materials. Clermont-Ferrand, France.
[49] W.J. Massman, Molecular diffusivities of Hg vapor in air, O2 and N2 near STP and the kinematic viscosity and thermal diffusivity of air near STP, ISSN: 1878-2442, Atmos. Environ. Volume 33 (Issue 3) (February 1999) 453–457, https://doi.org/10.1016/S1352-2310(98)00204-0.
[50] A. Reilly, O. Kinnane, F.J. Lesage, G. McGranaghan, S. Pavía, R. Walker, R. O'Hegarty, A.J. Robinson, The thermal diffusivity of hemplime, and a method of direct measurement, ISSN 0950-0618, Constr. Build. Mater. 212 (2019) 707–715, https://doi.org/10.1016/j.conbuildmat.2019.03.264.
[51] M. Rahim, O. Douzane, A.D. Tran Le, G. Promis, B. Laidoudi, A. Crigny, B. Dupre, T. Langlet, Characterization of flax lime and hemp lime concretes: hygric properties and moisture buffer capacity, ISSN 0378-7788, Energy Build. 88 (2015) 91–99, https://doi.org/10.1016/j.enbuild.2014.11.043.
[52] B. Mazhoud, F. Collet, S. Prétot, C. Lanos, Effect of hemp content and clay stabilization on hygric and thermal properties of hemp-clay composites, ISSN 0950-0618, Constr. Build. Mater. 300 (2021) 123878, https://doi.org/10.1016/j.conbuildmat.2021.123878.